Fire Technology, 47, 321–340, 2011

DOI: 10.1007/s10694-009-0134-4

Analysis on Downwind Distribution of Firebrands Sourced from a Wildland Fire

Hai-Hui Wang, Urban Systems Program, CSIRO Sustainable Ecosystems, P.O. Box 310, North Ryde, NSW 1670, Australia*

Received: 14 July 2008/**Accepted:** 14 December 2009

Abstract. Generation of firebrands from a wildland fire and their distribution downwind are studied using an analytical approach. The processes considered include emission of firebrands, wind-driven transport and the associated spot ignition. Emission of the firebrands from a fire front is treated as a stochastic process reflecting the interaction between gas flow plume and the burning fuel debris formed, with the emission rate being dominated by the rate of fuel consumption, emission factor and a function of firebrand sizes. Analogous to the random distribution of non-burning windborne particles, the transient distribution of firebrands downwind is described by a statistical pattern of Rayleigh form. Number and mass of firebrands landed downwind within the maximum travel distance are then determined by integration over the entire impact period during fire spread and burning-out processes. Application of the model to the bushfire occurred in Canberra, Australia in 2003 indicates that this model provides reasonable prediction in the distribution of firebrands downwind, and quantitatively exhibits the role of ember attack in massive destruction of houses at urban interface.

Keywords: Wildland fire, Firebrands, Number and mass distribution, Fire risk at urban interface

Nomenclature

A_s	Maximum cross-section area of a firebrand (m^2)
C_d	Drag coefficient of a firebrand in flowing air (0.45)
F_e	Firebrand emission factor for specific wildland fuels (kg^{-1})
g	Acceleration of gravity (m s^{-2})
$G(r_i)$	Rate of firebrands emitted from a fire source (m^{-2} s^{-1})
H_c	Heat of combustion of wildland fuels (18,620 kJ kg^{-1}) [1]
$h_{\max}(r_i)$	Height travelled by a firebrand with radius r_i (m)
I_b	Fireline intensity (kW m^{-1})
L_f	Flame length (m)
$M(x_i - x_0)$	Mass of firebrands distributed downwind at a location of $x_i - x_0$ (kg m^{-2})
m_{cr}	Critical mass of firebrands leading to successful ignition of the objects contacted (6.0 g)
$\dot{m}_f$	Fuel consumption rate in combustion zone determined by I_b/H_c (kg m^{-1} s^{-1})
$N(x_i - x_0)$	Number of firebrands distributed downwind at a location of $x_i - x_0$ (m^{-2})
$p(r_i, x)$	Distribution function of firebrands with radius between r_i and $r_i + dr_i$ (m^{-1})
P_f	Ignition probability of houses downwind

* Correspondence should be addressed to: Hai-Hui Wang, E-mail: HHWang4@ustc.edu.cn

r	Radius (m)
r_0	Brand radius with the highest frequency of appearance (0.012 m)
r_i	Brand radius (m)
r_{max}	Maximum loftable brand radius (m)
r_{min}	Minimum radius of lofted brands that play a role in igniting the objects contacted (m)
t	Time (s)
t_b	Entire impact period of fire spread and the subsequent fire burning out (s)
t_c	Burning duration of a firebrand (s)
t_r	Flame residence time (s)
t_s	Duration of fire spread (s)
U_g	Up-draught gas velocity (m s^{-1})
U_t	Terminal velocity of a firebrand at fall in still air (m s^{-1})
U_w	Environmental wind speed (m s^{-1})
v_f	Rate of fire spread (m s^{-1})
V_s	Volume of a firebrand (m^3)
x_0	Distance between the initial firefront and the edge of the vegetations or the targeted area (m)
x_i	Distance between a fire front and a target considered (m)

Greek symbols

β	A correction factor (0.7)
$\delta(r_i)$	A parameter in association with the function $p(r_i, x)$ (m)
η	A coefficient determined based upon experimental results of Tarifa et al. [2] (0.435 mm^2 s^{-1})
θ_f	Angle of flame surface to the vertical
λ	A constant determined based upon an experimental curve reported by Tarifa et al. [2] (2.86×10^{-4} s^{-2})
ρ_a	Density of ambient air (1.2 kg m^{-3})
ρ_s	Density of wildland fuels (542 kg m^{-3})
σ	A constant evaluated as 0.37
χ	A hardness factor for alive pine trees to liberate firebrands (0.15)

1. Introduction

'Spotting' is a common phenomenon in wildland fires. This phenomenon is characterised as the burning debris of wildland fuels lofted from the combustion zone and shifted by environmental wind to locations some distance away from a fire. The burning fuel debris landed, often named as firebrands or embers, may lead to new spot fires in the unburnt areas such as grassland, houses at wildland/urban interface and other inter-bushland facilities. For this reason, firebrand formation, transport and the subsequent spot ignition have been recognised as important processes in the study of bushfire behaviour and its impact at the urban interface.

Generation and transport of firebrands are primarily dominated by two mechanical forces driven by the up-draught gas flow formed around the burning fuels and the horizontal natural wind. Owing to the development of a buoyant plume, or the so-called convection column, around the combustion zone, burning fuel debris is lofted into the airstream, which may be present in pieces of tree leave or barks, segments of twigs, or seed shells, with sizes usually ranging from

millimetres to centimetres [1]. The firebrands are blown into the areas downwind, and then deliver energy to the unburnt objects contacted, contributing to the commencement of new fires.

Existing research related to the firebrand phenomenon has been focussed on topics such as mass change or size variation of firebrands during their flaming combustion or smouldering, transition between the combustion states, and the trajectories of firebrands during transport [2–8]. The flow dynamics of the combustion zone and the up-layer buoyancy plume has been analysed numerically using the momentum, mass conservation and gas law, which yields the equations for determining the rate of up-draught gas flow within a fire plume, maximum loftable size of firebrands, lofted height and the maximum travel distance of windborne materials downwind [3–8].

Although it has been often observed during indoor or field experiments that successful ignition of the objects contacted such as wood decks or pine needle fuel beds is essentially governed by the number (mass) of firebrands and their combustion state [3, 9–12], little work has been done in regard to the evaluation of density of firebrands scattered downwind. An early attempt was made by Muraszew [3] to quantify the number of firebrands distributed downwind, based upon an estimation of the potential number of firebrands generated and an assumption of linear pattern in the amount of firebrands deposited. Important features, such as random generation of the firebrands, their size distribution and the number distributed downwind, have not been considered in the model development. A field test on the number of firebrands deposited downwind does not support such linear pattern [13]. In the open literature [14–16], certain statistical patterns have often been reported in the study of air dispersion of windborne non-combustible dust. Based upon numerical simulation on the trajectories of several types of firebrands discharged from a fixed heat source, Himoto and co-workers [17] suggested a log-normal pattern for describing the scattering of firebrands fallen on the ground.

The aim of the present work is to develop a mathematical model to determine the density of firebrands distributed downwind, based upon the principals established for firebrand transport and the statistical knowledge developed for windborne materials. Focus is placed on the description of the processes, such as emission of firebrands from a fire source and their transient distribution downwind. The model established is then applied to interpret the fire phenomena appeared at the urban interface during the Canberra bushfire in 2003.

2. Model Development

A wildland fire is developed at the urban interface, as shown in Figure 1. Under the assistance of an environmental wind, the fire front with a constant frontline burning intensity approaches the urban area at a steady rate v_f. Firebrands are generated by the combustion of tree canopies and trunks, and transported downwind both by gas flow formed in the fire plume and the horizontal wind. The problem is depicted as a two-dimensional one.

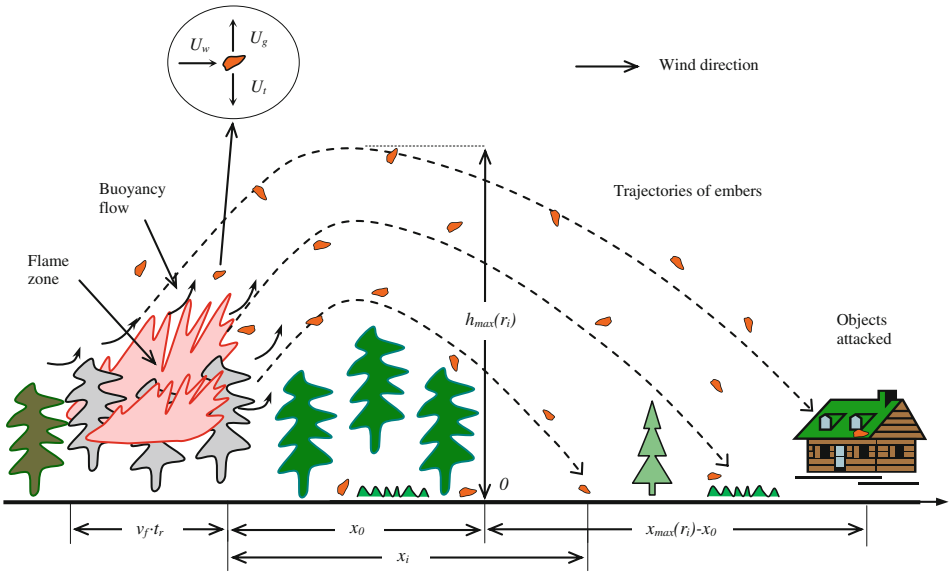

Figure 1. An illustration of the transport of firebrands and their distribution downwind.

Generation of firebrands is a random and dynamic process. As a result of combustion at various locations, segments of fuels are separated from the tree canopies and trunks, with some of them being lofted into the air due to strong up-draught gas flow formed in the fire plume. It has been often claimed by previous investigators [2, 5, 6] that the firebrands loftable within the fire plume must maintain sizes of less than a critical one with which terminal velocities of firebrands do not exceed the maximum plume velocity. The terminal velocities of firebrands indicate those maintained during the free drop of firebrands in still air, which are the function of the characteristic scale of firebrands [2, 4, 18]. Thus, we have the following inequality between the terminal velocities of firebrands and the gas flow rate in a fire plume

$$U_t = \sqrt{\frac{2\rho_s V_s g}{\rho_a C_d A_s}} \leq U_g \tag{1}$$

where V_s denotes the volume of a firebrand, A_s represents the maximum cross-section area of a firebrand, C_d signifies the drag coefficient of the firebrand, and g is the acceleration due to gravity. Parameter U_g is the rate of up-draught gas flow in the fire plume, which can be determined by the following empirical correlation [3]

$$U_g = 9.35\left(\frac{I_b}{H_c}\right)^{\frac{1}{3}} \tag{2}$$

where H_c stands for the heat of combustion of wildland fuels, that is 18,620 kJ kg^{-1} [1]. The parameter U_g has the units of m s^{-1}. Equation 2 has a form similar to that of Raupach [19] derived from a similarity theory.

As often reported in the literature [1, 2, 5, 6], typical firebrands may be presented in spherical, cylindric, or irregular shapes. For simplicity, the firebrands lofted in a fire plume are taken as spherical ones, then we have $V_s/A_s = r_i/3$. Thus, Equation 1 can be derived into a formula for determining the maximum loftable radius of firebrands $r_{\max}$, which has a form of $r_{\max} = 3\rho_a C_d U_g^2 \Big/ (2\rho_s g)$.

In general, any firebrands generated, by burning of trees, with diameters of less than the maximum loftable size are able to be dragged into the buoyancy plume. However, the particles with diameters of less than a critical value may play no role in the objects contacted downwind. This is because these particles are too small to maintain the flaming or glowing status during their travel and/or to make effective heat exchange with the objects contacted. If the total time period for firebrands to travel and to make effective heat exchange with the objects contacted is larger than 60 s [2, 3, 10], a firebrand necessarily to be taken into account in the present studies should own a radius of not being less than 5 mm. This determination for minimum firebrand radius is based upon an empirical correlation $t_c \approx r_i^2/\eta$, where η is evaluated as 0.435 mm^2 s^{-1} from the experimental data of Tarifa et al. [2].

As reported by Woycheese and co-workers [5, 6], the maximum loftable size of spherical firebrands can be correlated by parameters such as the heat release rate of a fire front, and physical properties of the solid fuels and the ambient air, whist the maximum loftable height of the firebrands can also be expressed in terms of the heat release rate of a fire front. By eliminating the heat release rate term from these two formulas, a relationship between the maximum loftable height and the maximum radius of firebrands can be developed into:

$$h_{\max}(r_i) = 1.46\left(\frac{\rho_s}{\rho_a C_d}\right)\left(\frac{r_{\max}^{2.5}}{r_i^{1.5}}\right) \tag{3}$$

where r_i stands for the radius of a firebrand and $r_{\max}$ denotes the maximum radius of the firebrands loftable in a fire plume. This equation concisely indicates a proportionality of $h_{\max}(r_i)$ to the reciprocal of the term $r_i^{1.5}$ [6].

Firebrand emission rate is evidently a function of the burning intensity of a fire; and hence the fuel consumption rate, although it may be closely related to the types of trees burnt and their growing status. In addition, the sizes of firebrands lofted from a fire source must not exceed the maximum loftable size. In light of the pattern observed for the particles emitted from residential wood log and pellet stoves [20], the rate of firebrands emitted from a fire source with the brand radius between r_i and $r_i + dr_i$ per unit width of the fire front and per unit time can be given by

$$G(r_i) = \frac{\dot{m}_f F_e}{r_i \sigma \sqrt{2\pi}} \exp\left[-\frac{1}{2\sigma^2}\left(\ln\frac{r_i}{r_0}\right)^2\right] \tag{4}$$

where $\dot{m}_f$ is the fuel consumption rate, kg m^{-1} s^{-1}, which can be directly worked out from the fireline intensity. Symbol F_e is an emission factor with a unit of kg^{-1}, specifying the number of potential firebrands generated from a fire source per unit mass of fuels. Symbol r_0 denotes the characteristic radius of firebrands, while σ is the so-called shape parameter. Parameters r_0 and σ are assumed to be independent of the fuel consumption rate and the emission factor. By considering the possible fireline intensity of up to 50 MW m^{-1}, maximum radius of firebrands possibly emitted from a fire source is determined, which allows a sensitivity analysis on the most possible value of radius r_0 for a range of values of parameter σ [20]. The parameter r_0 is then found to be 0.012 m, and the shape parameter σ is accordingly evaluated as 0.37.

When a fire front gets close to an urban area, it usually maintains a certain flame depth hence a quasi-steady fuel consumption rate. However, as long as it reaches the edge of a bushland, it will undergo a gradual decrease in flame depth till an occurrence of extinction as a result of complete consumption of the wildland fuels. The firebrand emission rates at these two distinct stages are then described by

$$G(r_i, t) = \begin{cases} G(r_i) & t \le t_s \\ G(r_i)\left(1 - \dfrac{t - t_s}{t_r}\right) & t_s < t \le t_b \end{cases} \tag{5}$$

where t_s denotes the duration of fire spread, and t_b is the total time prior to the fire burning out, which is actually the sum of duration of fire spread t_s and the fire residence time t_r.

Although there are no equations available in the literature for determining the transient distribution of firebrands deposited downwind from a fire source, the distribution pattern, in a statistical sense, should be at least somehow similar to that exhibited by the deposition of windborne heavy particles from a fixed, raised source. This hypothesis is based upon an understanding on the physics nature operated for these processes. As observed by Hage [14], the deposits downwind from a point source start from zero, increase significantly with distance, and decrease very gently after reaching the maximum, which can be described by a pattern of Rayleigh form. Noticing that the brands emitted from a fire source essentially undergo the drift within the ambient airstream after lofting, the frequency profile of firebrands with radius between r_i and $r_i + dr_i$ is then depicted by

$$p(r_i, x) = \frac{x}{\delta(r_i)^2} \exp\left[-\frac{x^2}{2\delta(r_i)^2}\right] \tag{6}$$

where the parameter $\delta(r_i)$ is defined as a function of maximum travel distance of firebrands, i.e. $\delta(r_i) = 0.153(x_{\max}(r_i))^{1.116}$. This is a constraint to ensure that the value of $p(r_i,x)$ will not exceed 10^{-4} for a brand to travel at a distance exceeding its maximum travel distance.

Maximum travel distances of firebrands are determined based upon the findings of Tarifa and co-workers [2] that in still air firebrands always fly at their final or terminal velocity of fall. Taking into account the horizontal distances travelled by firebrands within a fire plume (i.e. the convection column), the maximum travel distance for firebrands with radius between r_i and $r_i + dr_i$ can be written by

$$x_{\max}(r_i) = \beta h_{\max} \tan\theta_f + \frac{h_{\max} U_w}{U_t(r_i)} = h_{\max}\left(\beta \tan\theta_f + U_w\sqrt{\frac{3\rho_a C_d}{2\rho_s r_i g}}\right) \tag{7}$$

where θ_f represents the angle of flame to a vertical plane, which can be determined by an empirical correlation $\tan\theta_f = 1.35U_w(gL_f)^{-1/2} \approx 0.10U_w\dot{m}_f^{-1/3}$ [21, 22]. A correction factor β, evaluated as 0.7, is introduced here to moderate the overestimation of the distance travelled by firebrands within the convection column, by assuming an inclination of the column at an angle equal to the flame angle.

The number of firebrands per unit width at a distance x_i downwind is quantified by an integration over the range of brands with radius from $r_{\min}$ to $r_{\max}$ and throughout the entire impact period, i.e.

$$\begin{aligned} N(x_i - x_0) &= \int_0^{t_b}\int_{r_{\min}}^{r_{\max}} G(r_i,t)p(r_i,t)dr_i dt \\ &= \int_0^{t_b}\int_{r_{\min}}^{r_{\max}} \frac{G(r_i,t)(x_i - v_f t)}{\delta(r_i)^2}\exp\left[-\frac{(x_i - v_f t)^2}{2\delta(r_i)^2}\right]dr_i dt \end{aligned} \tag{8}$$

where x_0 is the distance between the initial fire front and the edge of the bushland, which is usually equal to $v_f t_s$.

Substitution of Equation 5 into Equation 8 yields a formula for determining the final distribution of firebrands accumulated during the period of fire spread and prior to fire burning out

$$\begin{aligned} N(x_i - x_0) = &\int_0^{t_s}\int_{r_{\min}}^{r_{\max}} \frac{G(r_i)(x_i - v_f t)}{\delta(r_i)^2}\exp\left[-\frac{(x_i - v_f t)^2}{2\delta(r_i)^2}\right]dr_i dt \\ &+ \frac{t_r(x_i - v_f t_s)}{2}\int_{r_{\min}}^{r_{\max}} \frac{G(r_i)}{\delta(r_i)^2}\exp\left[-\frac{(x_i - v_f t_s)^2}{2\delta(r_i)^2}\right]dr_i \end{aligned} \tag{9}$$

Utilising Equations 3, 4, 7 and 9, the density of the firebrands downwind can be evaluated numerically with the aid of a math tool. Input parameters include fireline burning intensity, local wind speed, rate of fire spread, and duration of fire spread. The emission factor is also a parameter required to be pre-set prior to the computations.

3. Results and Discussion

3.1. Size Distribution of Firebrands from a Fire Source and Rayleigh Distribution of Firebrands Downwind

In the model development, dependence of the transient emission rate of firebrands on their sizes is correlated by taking into account the results measured for the particles emitted from a fire stove [20], with a specific statistical function being included. It is obvious that generation of burning fuel debris is a random process, relying on tree structures, mechanical status of leave and twigs, burning intensity of trees, as well as the environmental wind conditions. Any fuel debris separated from the main parts of the burning trees should be loftable with the diameters below the maximum loftable size. Like other stochastic processes, the majority of firebrands should be constituted by the particles with moderate sizes, while those with the finest and maximum sizes should maintain very small portions in the number of firebrands emitted, due to the nature of combustion of these bio-fuels and the mechanism of up-lofting firebrands within a fire plume. An evidence to support this trend is given recently by Manzello and co-workers [12], who measured the dimensions of firebrands generated by burning of Douglas-Fir and Korean pine trees in still environment.

Typical frequency distributions of the firebrands downwind are evaluated using Equation 6 for various values of $\delta(r_i)$ and plotted in Figure 2. Individual curves specify the probabilities of firebrands distributed within their maximum travel distance for those with radius between r_i and $r_i + dr_i$ emitted from a source at time t. Since a large value of $\delta(r_i)$ corresponds to the brands with a small radius, the distribution of the brands with a large value of $\delta(r_i)$ may cover an extended area due to their light mass and accordingly small magnitudes in the terminal velocities U_t. On the contrary, the brands with a small value of $\delta(r_i)$ can only spread in a region close to the fire source, because of their large magnitudes in the terminal velocities. These trends coincide with the practical observations reported in the literature [2–4, 18].

The reasonableness of zero frequency at the start of the impact area is due to the fact that usually there exists a minimum distance for a firebrand to travel. As long as the firebrands stay in a fire plume, even at the edge of the fire plume, the gaseous buoyancy flow may always play a role in lofting the firebrands into the air, which has been well documented in the literature [5, 23]. It was also observed during the measurement of the dispersion of fluorescent-dyed glass microspheres with nominal diameter of 100 μm from a point source at a height of 15 m, that

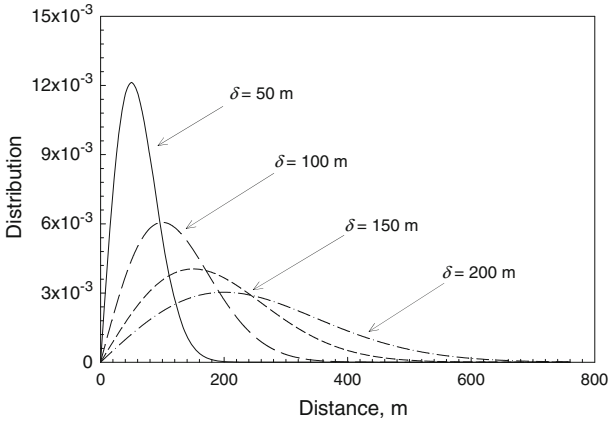

Figure 2. Profile of parameter $p(x)$ as a function of impact distance for various values of $\delta(r_i)$.

the deposition of particles becomes accountable only after a distance of more than 20 m downstream of the source [14].

There is no doubt that generation of firebrands from a fire source may be more or less affected by the properties of the burning trees especially the mechanical status of leave and barks prior to occurrence of a wildland fire, and the transport of firebrands essentially depends on up-draught gas flow, individual brand sizes, and the environmental wind speed. Nevertheless, the instantaneous distribution of firebrands downwind should follow a pattern similar to that exhibited by fine dust particles emitted from a raised, fixed source, since these two phenomena are identically dominated by the localised airflow dynamics rather than molecular diffusion process. As reported by Hage [14], the particle concentration distributed downwind starts from zero, followed by a sharp increase, and returns to zero gradually after reaching a peak. Analogous patterns were also reported for the firebrands, by tracing the trajectories of various types of firebrands discharged from a fixed heat source using a numerical approach with/without considering the combustion state of firebrands during travel [8, 17].

The asymmetric pattern in the distribution of firebrands across the impact area has taken into account the incapacity of firebrands prior to landing on specific objects. During their travel, the brand sizes reduce continuously due to persistent combustion occurred on individual brand surfaces. In addition, there is a tendency for a brand travelling over an extended distance to go to extinction because of a prolonged period of exposure to the cold convective environment. It is realistic to expect that the effective number of firebrands transported downwind should obey an off-central distribution rather than a symmetric one.

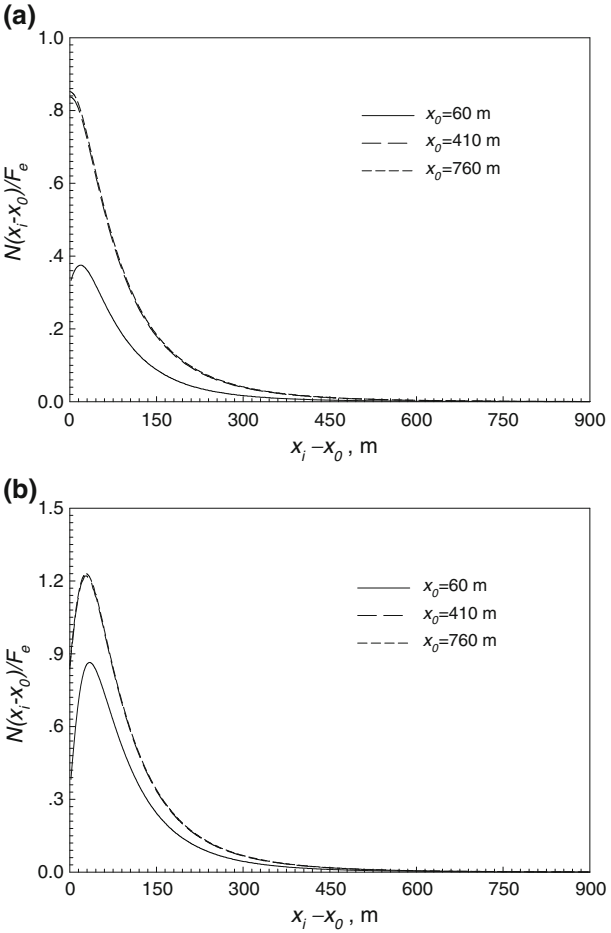

Figure 3. Distribution of $N(x_i)/F_e$ across the maximum travel distance during fire spread (a) and the period prior to the fire burning out (b). Calculations were done by setting U_w = 55 km h^{-1}, I_b = 48,063 kW m^{-1}, v_f = 11 km h^{-1} and t_r = 60 s.

3.2. Prediction of the Firebrand Density Downwind for Various Fire Intensities and Durations of Fire Spread

Dynamic accumulation of firebrands at various locations downwind is simulated by considering a fire front commenced at an initial distance x_0 from the edge of the impact area considered and quantifying the number of firebrands emitted and transported during the period of fire spread (Figure 3a). Calculations were done with the term $N(x_i - x_0)/F_e$, which allowed to avoid the evaluation of parameter F_e. The integrated distribution of firebrands at the end of a fire spread always exhibits

instantaneous drop by distance, starting from an elevated level. An increase in the initial distance x_0, corresponding to an extended period of ember attack, leads to a raised level in the number of firebrands accumulated in the impact area. However, the results are essentially identical for $x_0 \geq 410$ m, indicating that a fire front at the given burning intensity may make negligible contribution to the increase in the brand number at various locations downwind while the distance between the fire front and the edge of the impact area exceeds 400 m.

The number of firebrands distributed downwind as a result of bushfire attack throughout the period prior to the fire burning out has been determined by setting the flame residence time of 60 s, and is plotted in Figure 3b. Similar trends have been observed in regard to the distribution of the number of firebrands, although the inclusion of the firebrands emitted during fire burning-out process leads to a rise in the levels of the distribution curves. It is also found that the peak point in each curve slightly drifts from the edge of the vegetations due to the gradual diminishing depth of the burning zone and the shifted effective area of ember attack.

Number of firebrands accumulated at various locations downwind was also calculated for three distinct fireline intensities. The integrated number of firebrands, without considering the fire burning-out process, is shown in Figure 4a. The magnitude of the term $N(x_i - x_0)/F_e$ starts from an elevated level, and undergoes a drop with the increase in distance. For a fireline intensity of 1.35×10^4 kW m^{-1} (corresponding to a flame length of 15 m), it becomes negligible at a distance exceeding ~50 m. With an increase in the fireline intensity, the level of the curve is raised. For a burning intensity equal to 4.81×10^4 kW m^{-1} (corresponding to a flame length of 35 m), the number of firebrands per square meters turns to be minor only at a distance exceeding ~500 m.

Similar pattern has been observed in the number of firebrands distributed downwind prior to the fire burning out, as shown in Figure 4b. The lower peak value in the curve for the largest fireline intensity may be attributed to the shorten fire residence time set according to a rule $t_r \propto I_b^{-1}$ [24].

The trend of firebrand distribution is essentially in agreement with the field test results reported by a CSIRO bushfire research group [13]**.** As shown in Figure 4, the continuously-decreasing pattern can be approximated by an exponential function in general especially for a fireline intensity of around 2.90×10^4 kW m^{-1}. For comparison, it was observed that the number of firebrands emitted from the roofs of burning shops or residential areas undergoes abrupt decrease by the distance downwind, as described in an internal technical report of IIT Research Institute [25].

As discussed previously, under any circumstances a brand should only be harmful while its radius is not less than 0.005 m, so as to have sufficient time to make a travel and to complete heat exchange with the object contacted. This leads to a formula for determining the minimum fireline intensity needed for an effective ember attack, i.e.

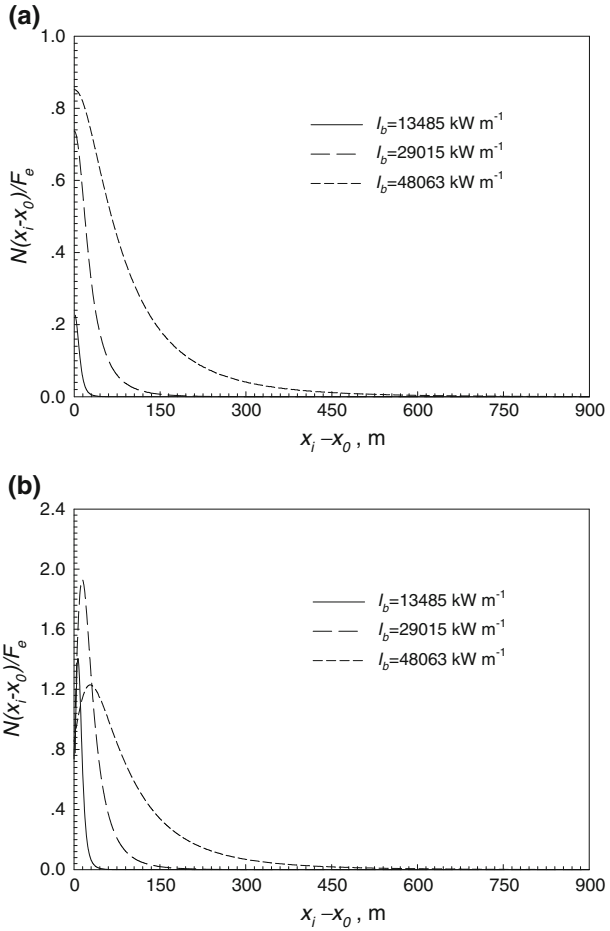

Figure 4. Profile of the function $N(x_i)/F_e$ for various fireline intensities during fire spread starting at a distance of 760 m to the urban edge (a) and prior to fire burning out (b). Parameter inputs include: (1) U_w = 30 km h^{-1}, v_f = 3 km h^{-1}, t_r = 180 s and I_b = 13485 kW m^{-1}; (2) U_w = 40 km h^{-1}, v_f = 6.5 km h^{-1}, t_r = 84 s and I_b = 29015 kW m^{-1}; (3) U_w = 55 km h^{-1}, v_f = 11 km h^{-1}, t_r = 60 s and I_b = 48063 kW m^{-1}.

$$I_b \geq H_c \left(\frac{\rho_s g r_{\min}}{131.13 \rho_a C_d} \right)^{\frac{3}{2}} \tag{10}$$

A minimum value of 4.28×10^3 kW m^{-1} is then found for the parameter I_b by inputting pre-set values of the other parameters in Equation 10. This value implies the critical fireline intensity for which a non-harmful delivery of firebrands may

occur. In other words, once fireline intensity is less than 4.28×10^3 kW m^{-1}, the firebrands lofted by gas flow within a fire plume may only have impact on the adjacent areas at a distance of several meters at most due to the limited number of firebrands transported and short burning span for such small-sized brands. This critical fireline intensity corresponds to a fire with a flame length of 7 m, which is in excellent agreement with the conditions under which a spot fire is likely to occur, as suggested by Alexandrian [26], based upon an investigation on the past 201 fires occurred in European and Mediterranean countries.

3.3. Analysis on the Role of Ember Attacks Occurred in Duffy Area During Canberra Bushfire in 2003

The house destruction in the Duffy residential area in 2003 is a typical example of ember attack during a wildland fire. As observed during the bushfire development and the post-fire investigation [27, 28], embers sourced from the burning of pine trees in the adjacent bushland were blown into the urban area by local wind, resulting in ignition and subsequent destruction of houses in number of locations within a distance of up to 550 m from the edge of vegetations. The number of embers that landed downwind during the bushfire development can be simulated using the model established. Parameters utilised in the computations are shown in Table 1.

Rate of fire spread was estimated based upon the data of McRae [31]. Flame residence time was evaluated by taking into account the fireline intensity and the general fuel loading reported by McRae [31]. The emission factor is estimated using a formula suggested by Muraszew [3], that is $\chi\psi_a^3/(16\pi\kappa_a\rho_s)$, where ψ_a stands for the surface to volume ratio of firebrands, ρ_s denotes the density of the so-called dead fuels, κ_a signifies firebrand length to diameter ratio, and χ is introduced here as a hardness factor for alive pine trees to liberate firebrands, which is set at 0.15. For the spherical firebrands, the potential number of firebrands pro-

Table 1
Parameters Evaluated for Simulating Firebrand Transport at the Urban Interface in Duffy Area During Canberra Bushfire 2003

Parameter	Value	Comment
x_0 (m)	560	Determined from the ACT geological and vegetation map
U_w (km h^{-1})	55	Quoted from the literature [23, 29, 30]
I_b (kW m^{-1} s^{-1})	48,063	Evaluated from the flame length recorded in the video of ACT bushfire 2003 [23, 27]; data reported by Chen and McAneney [29]
v_f (km h^{-1})	11	Evaluated from the bushfire behaviour described by McRae [31] and a linearity of the fire burning intensity to the rate of fire spread
t_r (s)	60	Estimated from the video taped during the bushfire occurred at urban interface in Duffy area [27]
F_e (kg^{-1})	68	Calculated based upon a method of Muraszew [3] and in reference to the test results of Manzello et al. [11]
m_{cr} (g)	6.0	Assumed based upon the experimental data reported by Dowling [9] and Manzello et al. [10]

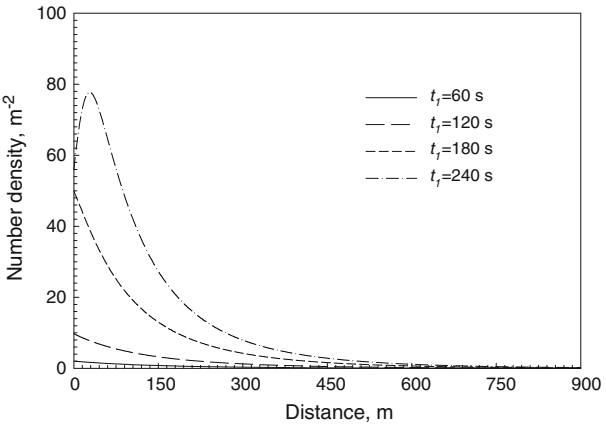

Figure 5. Number of firebrands accumulated at various distances downwind during the fire spread and burning-out processes. Calculations were done with the parameters reported in Table 1.

duced with average radius of 0.013 m is ~68 kg^{-1} during the burning of wildland fuels with a density of 542 kg m^{-3}. This evaluation was not accurate since the impact of local wind speed and fuel types on the formation of firebrands has not been taken into account. Worthy of mentioning, in the study of the dispersion of wind-borne materials, the emission rate has been named as source strength, and has always been pre-set prior to the modelling [15, 16].

The number of firebrands landed at different locations in the urban area was quantified and shown in Figure 5. At a specific time during ember attack, the number of firebrands demonstrates a continuous decrease along the distance with the maximum being always at the positions close to the edge of bushland. Prior to the fire burning out, the level of firebrands per square meters landed downwind is getting reasonably high, with the maximum reaching ~77 at a location very close to the edge of vegetation. Indirect evidence to support the above prediction is that isolated burnt spots were often observed on house components and in the garden during the investigation of over 220 houses and their surroundings in the area within a distance of <400 m to the urban edge [28, 32]. These burnt spots were found to be on the roofs, at the corner of window frames and doors, as well as on the surface of decks and fence, and are usually present in irregular shapes, with the burnt areas varying from ~0.1 cm^2 to ~10,000 cm^2 [32]. These observations at least somehow reflect the impact of the ember attack as a result of the wildland fire spread in the adjacent area, although we cannot rule out the impact of the embers sourced from the adjacent house fire and garden fire.

The predicted density of firebrands distributed downwind is in qualitative agreement with the field test results for the firebrands emitted from the roof of a burning small-scale shop, reported by Vodvarka [25]. Worthy of mentioning, a total of 75,367 brands were recorded by Waterman [33] during the measurement by burn-

ing wooden high-pitch roof with the roof area of 8.46 m^2 in a fire chamber, under the enhancement of an upward wind at a speed of 6.7 m s^{-1}. These brands constitute a mass of ~6.95 kg, which were sourced from the burning of a mass of around 70 kg prior to the collapse of the roof sample with an initial mass of ~116 kg (estimated using an assumed wood density of 542 kg m^{-3}). In contrast, in a recent burning of Douglas-Fir trees in still environment [11], a loss of more than 10 kg only yields a production of firebrands being not more than 50 g. It seems that, the mechanism of lofting (up-draught gas flow) in the combustion zone plays an important role in the generation of firebrands, while burning of individual small-sized tree crowns in still environment may not create such mechanism. This hypothesis has been confirmed by the experiments carried out in the combustion wind tunnel, where enormous burning or burnt particles were generated during burning of pine needles in the fuel bed in a windy environment [34].

Landing of firebrands does not automatically imply the commencement of spot fires and the subsequent burning of houses, as often observed during the post-fire survey [32]. In fact, spot ignition is a phenomenon governed by several factors, with the most important being the mass of embers gathered. Dowling [9] reported that a mass of more than 7 g of embers is required to lead to the ignition and sustainable smouldering of a timber deck during tests with decking structures. Manzello and co-workers [10] carried out experiments with the deposition of glowing embers (machined *Pinus ponderosa* pine wood discs) on the fuel bed with an area of 23 × 23 cm^2, and found that the minimum mass for igniting various types of combustibles, such as pine needles, shredded paper and cedar shingles, varies from 1.5 g to 6.0 g. Thus, a simple method for finding out the locations where the ignition and the sustainable combustion could occur as a result of the ember attack may lie between the quantification of the mass of embers landed on specific areas and the assessment on whether the mass of firebrands meets the requirement for igniting the objects contacted.

Although the total number of firebrands is conserved till their landing on the impact area, firebrands may undergo mass loss during travel. The combustion experiments with spherical and cylindrical firebrands of different sizes and with five types of wood materials show that the mass variation of firebrands with time can be described by an empirical equation $\rho/\rho_s = 1/(1+\lambda t^2)$ [2]. By utilising this equation, the mass of firebrands per square meters distributed at a specific location downstream at time t_1 is determined by

$$M(x_i - x_0) = \int_0^{t_1} \int_{r_{\min}}^{r_{\max}} \frac{4\pi r_i^3 \rho_s G(r_i, t)(x_i - v_f t)}{3(1+\lambda t^2)\delta(r_i)^2} \exp\left[-\frac{(x_i - v_f t)^2}{2\delta(r_i)^2}\right] dr_i dt \tag{11}$$

where λ is a parameter related to the fuel type, evaluated as 2.86×10^{-4} s^{-2}, based upon the experimental data of Tarifa and co-workers [2]. Note that in the above calculation mass change of firebrands during travel has not been fully considered, especially for those emitted at a time close to t_1. However, the error introduced is essentially negligible once the impact time t_1 is far larger than the time

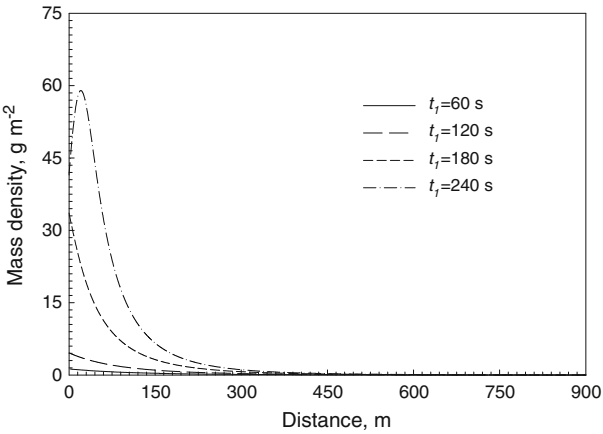

Figure 6. Mass of embers accumulated at various distances downwind during the ember attack at different time intervals. Parameters evaluated in the calculations were the same as those in Figure 5.

for a firebrand to travel prior to its landing onto a target (i.e. <40 s in general at a local wind speed exceeding 30 km h^{-1}).

Mass of firebrands distributed downwind at different times is calculated and plotted in Figure 6. With the fire front approaching the urban interface, there is simultaneous accumulation in the mass of firebrands in the urban area. However, in the first 60 s, within the region attacked the ember density is fairly low with the maximum being about 1.2 g m^{-2}. This situation has only been changed slightly in 120 s. After a period of 180 s, mass density of firebrands rises significantly, especially within a distance of ~120 m from the edge of wildland vegetations. By taking into account the brand gathering effect, we can expect that in number of positions within 120 m from the edge the brand mass accumulated may exceed the threshold for igniting the objects contacted, which is about 6.0 g for specific combustibles located in the urban areas. Prior to the fire burning out, this region is extended to an area at a distance of up to 160 m as a result of continued ember attack.

The mass density information can be more easily interpreted by converting it into the ignition probability of houses located at the urban interface via the following formula

$$P_f(x_i - x_0) = \begin{cases} \dfrac{M(x_i - x_0)}{m_{cr}} & M < m_{cr} \\ 1 & M \geq m_{cr} \end{cases} \tag{12}$$

where m_{cr} denotes the minimum mass required for embers to ignite an object contacted. A concept of self-gathering of embers in unit areas during landing is utilised in the above equation. This concept was often adopted in the laboratory tests for studying the impact of firebrands on ignitable materials [9–12]. As

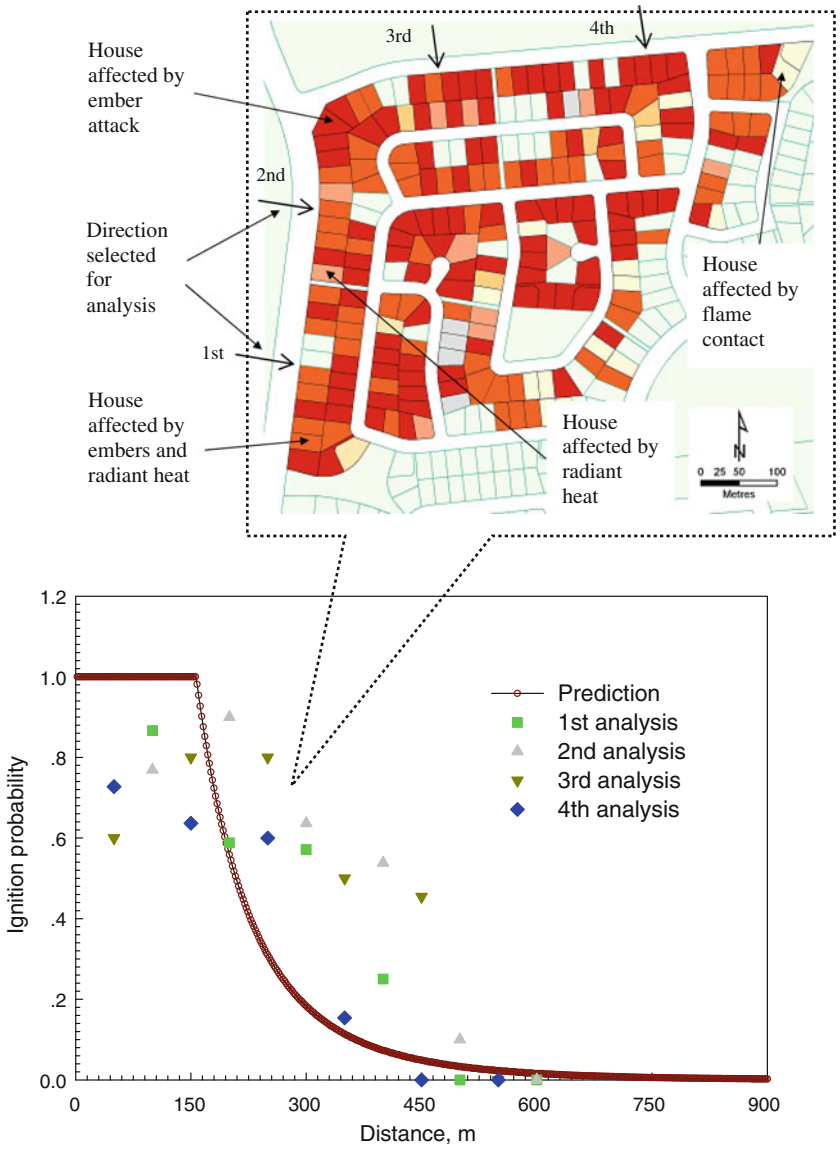

Figure 7. Comparison of the ignition probability predicted using the present model with the percentages of houses affected by ember attack in Duffy area [28]. Percentage of houses affected was sampled in four different regions (directions) starting from the edge of vegetations, and the density of houses corresponding to an individual central position was practically determined by counting the houses in a rectangular cell with the area of 100 × 100 m².

observed during a post-fire survey [32], embers were often accumulated in specific positions, such as deck gaps, fence bases, window/door corners, and it was such phenomenon that eventually leads to successful spot fires.

As shown in Figure 7, the ignition potential of the houses within a distance of about 160 m from the edge of wildland vegetations always maintains unity due to extensive attack of embers sourced from burning of the strip of pine trees in the adjacent areas. On the other hand, with the increase in distance, the probability drops drastically and almost reaches zero at a distance of ~600 m. This prediction has been in good agreement with the results of the percentages of houses affected by ember attack at various locations determined by a post-fire survey [23, 28].

Note that the surveyed results may contain errors due to the difficulties in accurately identifying the reasons responsible for the damage of some of the houses during the fire, which can be partially attributed to the three parallel ignition mechanisms operated at the urban interface (refer to Figure 7). For instance, the lower percentages of the houses affected by ember attack in the area very close to the wildland fire may be due to the fact that direct flame contact and the radiation sourced from the wildland fire may sometimes become the dominant mechanisms leading to house damage. However, this does not mean that these houses affected by direct flame contact and fire radiation were never suffered from the attack of embers formed by burning of wildland fuels. As revealed by further investigations on the residential fire in Duffy area [30], some of the houses were lit by the embers sourced from neighbouring house fire or garden fire rather than directly from the wildland fire. This should also explain the disparity between the model predictions and the surveyed percentages of houses affected by the ember attack in the region at a distance of between 200 m and 400 m from the edge of vegetations.

The simulated results essentially have significance in drawing an overall picture for ember attack at the urban interface and in revealing the reasons for the random distribution of houses affected in the urban areas [23]. A successful spot ignition is not only dependent to the mean density of embers accumulated in specific areas, but also the structure and properties of the objects contacted. A secondary fire may much easily be set on those combustibles that allow embers to land and to gather together. For these reasons, a more accurate prediction on the spot-fire phenomena should rely on a better description of the trajectories of firebrands in variant wind environment by taking into account the impact of downstream object structure, and of the conditions for initiating a spot ignition on an object with certain flammability.

4. Concluding Remarks

A mathematical model has been developed to quantify the number and mass of embers accumulated at various locations downwind during the attack of a wildland fire developed at a specific rate of fire spread and fireline intensity. Examination of the features of the model indicates that during the period of fire spread and prior to the fire burning out, the number of firebrands landed per square

meters downwind essentially follows a continuously-decreasing pattern across the impact area. Application of the model to the interpretation on the role of firebrands in house destruction at the urban interface during the Canberra bushfire in 2003 shows that the model provides realistic predictions in the number and mass of firebrands transported downwind at the urban interface, and explains the pattern of houses affected in Duffy suburb. For the first time, the model developed makes it available to determine the distribution of firebrands under various bushfire scenarios. There is potential to develop a tool based upon this model for assessing fire risk at urban interface due to the ember attack.

References

1. Pyne SJ, Andrews PL, Laven RD (1996) Introduction to wildland fire, 2nd edn. Wiley, New York
2. Tarifa CS, Del Notario PP, Moreno FG (1965) On the flight paths and lifetimes of burning particles of wood. In: Proc. of Tenth Symp (Inter) on Combust, The Combustion Institute, Pittsburgh, PA, pp 1021–1037
3. Muraszew A (1974) Firebrand phenomena. Aerospace Report No. ATR-74(8165-01)-1. The Aerospace Corp., El Segundo, CA
4. Albini FA (1979) Spot fire distance from burning trees—a predictive model. USDA Forest Service General Technical Report INT-56. Intermountain Forest and Range Experiment Station, Ogden, UT
5. Woycheese JP, Pagni PJ, Liepman D (1997) Brand lofting above large-scale fires. In: Proc 2nd Inter Conf on Fire Res and Eng, Society of Fire Protection Engineers, Boston, MA, pp 137–150
6. Woycheese JP, Pagni PJ, Liepmann D (1999) Brand propagation from large-scale fires. J Fire Prot Eng 10(2):32–44
7. Ellis PF (2000) The aerodynamic and combustion characteristics of Eucalypt bark—a firebrand study. PhD thesis, Australian National University, Canberra, ACT, Australia
8. Sardoy N, Consalvi JL, Kaiss A, Fernandez-Pello AC, Porterie B (2008) Numerical study of ground-level distribution of firebrands generated by line fires. Combust Flame 154(3):478–488
9. Dowling VP (1994) Ignition of timber bridges in bushfires. Fire Safety J 22:145–168
10. Manzello SL, Cleary TG, Shields JR, Yang JC (2006) On the ignition of fuel beds by firebrands. Fire Mater 30(1):77–87
11. Manzello SL, Maranghides A, Shields JR, Mell WE, Cleary TG, Yang JC (2006) Firebrand production from burning vegetation. In: Proc. 5th Inter Conf on Forest Fire Research, Luso, Coimbra, Portugal
12. Manzello SL, Maranghides A, Shields JR, Mell WE, Hayashi Y, Nii D (2007) Measurement of firebrand production and heat release rate (HRR) from burning Korean pine trees. In: Proc. 7th Asia-Oceania Symp on Fire Sci & Tech, Hong Kong Polytechnic University, Hong Kong
13. CFFP (2001) Project Vesta: Spotfire project, Bushfire behaviour and management, CSIRO Forestry and Forest Products, Kingston, ACT, Australia. http://www.ffp.csiro.au/nfm/fbm/vesta/spotfire.html. Accessed 2006
14. Hage KD (1961) On the dispersion of large particles from a 15-m source in the atmosphere. J Meteor 18:534–539

15. Pasquill F (1974) Atmospheric diffusion. The dispersion of windborne material from industrial and other sources, 2nd edn. Ellis Horwood Limited, Chichester, England
16. Hashem A, Parkin CS (1991) A simplified heavy particle random-walk model for the prediction of drift from agricultural sprays. Atmos Environ 25A(8):1609–1614
17. Himoto K, Tanaka T (2005) Transport of disk-shaped firebrands in a turbulent boundary layer. In: Proc. of 8th Symp on Fire Safety Sci, IAFSS, Beijing, China, pp 433–444
18. Clements HB (1977) Lift-off of forest firebrands. USDA Forest Service Research Paper SE-159. Southeastern Forest Experiment Station, Asheville, NC
19. Raupach MR (1990) Similarity analysis of the interaction of bushfire plumes with ambient winds. Math Comput Modelling 12(12):113–121
20. Boman C, Pettersson E, Nordin A, Westerholm R, Boström D (2006) Gaseous and particulate emissions from residential wood log and pellet stoves—experimental characterization and quantification. To be published
21. Thomas PH (1971) Rates of spread of some wind-driven fires. Forestry 44:155–175
22. Pagni PJ, Peterson TG (1974) Flame spread through porous fuels. In: Proc. 14th Symp (Inter) on Combustion, The Combustion Institute, Pittsburgh, PA, pp 1099–1107
23. Wang H-H (2006) Ember attack: its role in the destruction of houses during ACT Bushfire in 2003. In: Proc Bushfire Conf 2006—Life in a Fire-prone Environment: Translating Science into Practice, Griffith University, Brisbane, Queensland, Australia
24. Alexander ME (1982) Calculating and interpreting forest fire intensities. Can J Bot 60:349–357
25. Vodvarka F (1969) Firebrand field studies. IIT Research Institute Final technical report, Project J6148, Chicago, IL
26. Alexandrian D (2002) A probabilistic model for forecasting spot fires. In: Proc. 4th Inter Conf on Forest Fire Res and 2002 Wildland Fire Safety Summit, Luso, Coimbra, Portugal
27. Moran R (2003) Canberra firestorm: 18th January 2003. Channel 9 News Bureau, Canberra, ACT, Australia
28. Blanchi R, Leonard JE (2005) Investigation of bushfire attack mechanisms resulting in house loss in the ACT bushfire 2003. Report for Bushfire CRC, CSIRO Manufacturing and Infrastructure Technology, Highett, VIC, Australia
29. Chen K, McAneney J (2004) Quantifying bushfire penetration into urban areas in Australia. Geophys Res Lett 31:L12212
30. Doogan M (2006) The Canberra firestorm: inquests and inquiry into four deaths and four fires between 8 and 18 January 2003. ACT Coroners Court, ACT, Australia
31. McRae RHD (2004) The breath of dragon–Observations of the January 2003 ACT Bushfires. Emergency Services Bureau, ACT, Australia
32. Livbom A (2005) Fire phenomena at wildland/urban interface: an analysis based on post fire survey of Canberra Fire 2003. Industrial placement report for final-year university study in Sweden, CSIRO Manufacturing and Materials Technology, Highett, VIC, Australia
33. Waterman TE (1969) Experimental study of firebrand generation. IIT Research Institute Final technical report, Project J6130, Chicago, IL
34. Wang H-H, Zhang L-H, Liu N-A (2006) Impact of wind on the geometries and temperature profiles of fire plumes formed in bushfires. A Scientific Visit funded by Australian Academy of Science and China Academy of Sciences, State Key Lab of Fire Science, Univ of Sci & Tech of China, Hefei, Anhui, China